Evanescent-Wave Cavity Ring-Down Investigation of Polymer/Solvent Interactions

Theresa E. Hannon, Soonwoo Chah, and Richard N. Zare*

Department of Chemistry, Stanford University, Stanford, California 94305-5080

Received: January 4, 2005; In Final Form: February 12, 2005

Evanescent-wave cavity ring-down spectroscopy (EW-CRDS) is used to measure interfacial phenomena when methanol or water is placed in contact with a film of poly(dimethylsiloxane) (PDMS), which is attached to the face of a fused-silica prism that constitutes part of a ring cavity. In the first few minutes after contact, the uptake of methanol is slower than that of water, but after this initial period the methanol diffuses more rapidly in the film than water does. Bulk weight-gain measurements confirm this result and yield diffusion coefficients of $(25.1 \pm 0.7) \times 10^{-7}$ cm^2/s for methanol in PDMS and $(7 \pm 2) \times 10^{-7}$ cm^2/s for water in PDMS. The interfacial optical losses found in the EW-CRDS measurements result primarily from scatter. In particular, we find that delamination of the film from the fused-silica substrate dominates the optical losses in the case of methanol. This conclusion is confirmed by separate surface plasmon resonance experiments.

Introduction

Buried interfaces commonly occur in many practical devices, but the study of what happens at these interfaces is challenging, if not formidable, because of their hidden character. One way to examine such interfaces is to measure the attenuation of evanescent waves. This task is usually undertaken by recording attenuated total reflectance (ATR), but this technique typically employs a waveguide and the quantity measured is not localized. We use an alternative approach based on cavity ring-down spectroscopy (CRDS). This approach has the advantage that the same spot in the buried interface is repeatedly probed.

CRDS is an ultrasensitive spectroscopic technique in which the sample of interest is placed within a high-finesse optical cavity typically formed by highly reflective mirrors.[1−3] Light is injected into the cavity and makes numerous passes through the sample. The intensity of the light escaping the cavity decays exponentially and has a characteristic 1/e lifetime τ. The values of τ before and after introduction of the sample into the cavity can be used to calculate the optical attenuation caused by the sample.[4] Historically, this technique has been primarily used to measure very small optical losses in the gas phase. Recently, the technique has been extended to condensed-phase samples, with an emphasis on the design of instrumentation that minimizes nonsample optical losses such as reflection or absorption of light by a glass cuvette and therefore maximizes the empty-cavity ring-down lifetime.[5−20] Evanescent-wave cavity ring-down spectroscopy (EW-CRDS)[7,9,11,14,20] combines the CRDS technique with the standard surface-selective ATR method. In EW-CRDS, an optical element such as an antireflection-coated prism is placed within the optical cavity. The light enters the prism and undergoes total internal reflection (TIR) at the interface between the prism and a medium of lower refractive index such as a liquid solution or a polymer film. At this TIR interface, an electromagnetic field called an evanescent wave is formed and penetrates a short distance d_p (typically a fraction of a wavelength) into the lower-index medium. If an absorber or scatterer is placed at the interface, the reflected light is correspondingly attenuated.[21,22] For a ring cavity as described in this study, the interfacial optical loss per pass of the light onto the sample (A^*) can be calculated by using the equation

$$A^* = \frac{t_r(\tau_0 - \tau)}{\tau_0 \tau} \tag{1}$$

where t_r is the round-trip time of the light within the cavity, τ_0 is the ring-down lifetime for the background, and τ is the ring-down lifetime with the analyte of interest present. The variable A^* is used in this case to designate that the losses reported here do not necessarily result from absorption.

For the pulsed EW-CRDS system employed in this study, the current detection limits are comparable to those achieved with a waveguide ATR apparatus.[23] Despite the lack of an optical cavity, high sensitivity is achieved in ATR by passing the light along a length of thin glass sheet or a fiber optic at angles suitable for TIR, thereby forming many evanescent waves along the length of the waveguide. The major advantage of this particular EW-CRDS system over ATR is the potential for spatially resolved measurements. The EW-CRDS incident light hits the same point at the TIR interface on each bounce, achieving a confined optical loss measurement with spatial resolution that is limited only by the spot size of the incident light. This spatial advantage may prove useful for the study of interfacial systems with localized differences and provides motivation for the further refinement and application of the EW-CRDS technique. Recent studies have applied EW-CRDS to the analysis of thin films[7,24−27] and liquid systems.[14,20,28] In this study we extend EW-CRDS to the investigation of optical changes at a fused-silica/polymer interface as solvents diffuse into the thick polymer layer (thickness $\gg d_p$).

We have chosen to investigate the diffusion of methanol and water through the elastomer poly(dimethylsiloxane) (PDMS) whose chemical structure is shown in Figure 1. PDMS is employed in the construction of microfluidic devices for the analysis of single cells,[29] and it has been observed that diffusion of solvents and analytes through this polymer presents a significant limitation for the use of these devices.[30] There exists the possibility that EW-CRDS could be used to monitor the diffusion of solvents through specific areas of an individual chip

* Address correspondence to this author. E-mail: zare@stanford.edu.

10.1021/jp050045s CCC: $30.25
Published on Web 03/25/2005

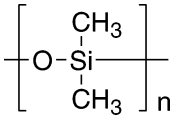

Figure 1. Chemical formula for poly(dimethylsiloxane).

that have been chemically modified to reduce permeation by particular reagents.

Here we use EW-CRDS to monitor the time evolution of the optical losses at a fused-silica/PDMS interface as methanol or water diffuses into the polymer. We observe significant interfacial optical losses that increase as each solvent penetrates the polymer and reaches the interface. We approach this study with two primary concerns. First, we want to determine what the EW-CRDS studies can tell us about diffusion coefficients. We show that the EW-CRDS experiments provide reasonable qualitative estimates of relative diffusion rates for the systems under investigation; however, we demonstrate that the interfacial optical losses result from scattering and are not sufficiently straightforward to provide quantitative diffusion coefficients. Therefore, we employ the traditional, nonspatially resolved weight-gain method to provide more exact bulk diffusion coefficients for comparison. Second, we want to elucidate the details of the physical process that causes such large optical losses at the buried prism/polymer interface. With the aid of surface plasmon resonance (SPR) experiments, we determine that the mode of polymer film delamination from the prism surface is the primary factor that dictates the magnitude of the scattering losses observed with EW-CRDS. Inhomogeneous delamination of PDMS by methanol causes large losses, whereas insertion of a thin, homogeneous film of water between the PDMS and the prism causes smaller attenuation of the EW-CRDS signal.

Experimental Methods

EW-CRDS Apparatus. Figure 2 depicts the optical cavity used to investigate solvent diffusion into PDMS by EW-CRDS. A dye laser (Quanta-Ray PDL with Exciton pyrromethene 597 dye) pumped by 532-nm radiation from a pulsed Nd:YAG laser (Spectra-Physics Pro-250) at 10 Hz produces the incident light at 600 nm. This radiation is apertured twice before injection into the optical cavity; no other spatial filtering of the beam was determined to be necessary for these experiments. The ring cavity consists of two high-reflectivity mirrors (Newport Ultra-Low Loss SuperMirrors; 1-m ROC; $R > 99.97\%$) and a custom-designed triangular prism[27] (Rocky Mountain Instrument Co.) that functions as the total internal reflection element and is mounted on a combination tilt/rotation stage (Newport, P046BL-50). To achieve suitably low optical losses, the prism was designed to minimize the light path through the substrate, was constructed from UV-grade fused silica (Corning 7980), and was coated on the input and output faces with a state-of-the-art antireflective coating ($R < 0.03\%$). Aligning the mirrors at an angle θ of $\sim 11.8°$ provides an angle of incidence within the prism ($\varphi \approx 75.6°$) that is appropriate to provide TIR for the polymer samples described below. A simple Plexiglas cell (~ 0.3 mL) is used for injection of liquid samples above the TIR surface. The cell is secured to the prism with a plastic O-ring and pressure from screws that are attached to the prism mount.

A 600-nm, narrow-band notch filter (CVI Laser) and a metal tube are placed after the cavity to block amplified spontaneous emission of different wavelengths from reaching the detector; in addition, a ground-glass diffuser plate is positioned directly in front of the detector to minimize the effects of mode beating

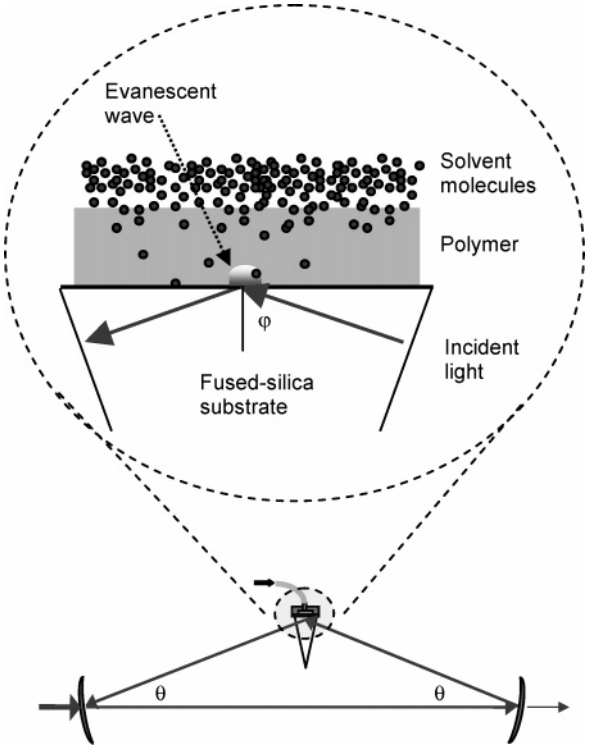

Figure 2. Optical cavity used for the EW-CRDS experiments, containing the triangular prism with attached flow cell. The inset shows a representation of the polymer/prism interface. These diagrams are not drawn to scale.

on the measured ring-down profile, as suggested by Pipino, Hudgens, and Huie.[7] The light exiting the cavity through the second mirror is detected by a photomultiplier (Hamamatsu Corporation, R4632). The exponential decay envelope (the ring-down) of this light intensity is visualized on an oscilloscope (LeCroy, LT342) and is analyzed with LabVIEW software (National Instruments) to determine the value of the ring-down lifetime τ. The standard LabVIEW exponential fitting routine is found to give the same results as a Levenberg−Marquardt fit, within error. Without a sample on the back of the prism, this setup produces ring-down lifetimes of approximately 900 ns.

EW-CRDS Investigations. To prepare PDMS films for study by EW-CRDS, GE Silicones components RTV615A (linear polymer) and RTV615B (containing cross-linking agent) were combined in a 10:1 (w:w) ratio and mixed thoroughly for approximately 2 min. The mixture was degassed in a vacuum desiccator for about an hour; it was then spin coated onto glass microscope slides that had been cleaned by wiping twice with acetone and toluene, respectively. We cured the polymer film at 80 °C for 3 h. Polymer film thicknesses ranged from 167 to 387 μm, which is much greater than the penetration depth of the evanescent wave; we measured thicknesses for specific films following the EW-CRDS measurements as described below.

For each experimental EW-CRDS trial, a piece of PDMS film (~ 2 cm $\times$ ~ 3 cm) was peeled off the microscope slide and placed on the cleaned TIR surface of the prism, taking care to avoid as much as possible air bubbles and dust particles. The optical quality of the polymer/prism interface at the laser spot was determined by the ring-down lifetime that is achieved with the film in place. Interfaces for which the ring-down lifetime exceeds 570 ns were deemed to be sufficient for EW-CRDS study and subsequent analysis. Others were too optically lossy, and we attributed these losses to scattering by structural inhomogeneities between the polymer layer and the prism. For

example, the presence of a dust particle or a small air bubble at the interface should cause it to be susceptible to changes in optical quality with the exertion of pressure on the polymer or with swelling of the polymer.

After the polymer was placed on the prism surface, the liquid cell was secured to the polymer. An aliquot of methanol (Mallinckrodt SpectrAR) or water (Millipore Milli-Q UV Plus, 18 MΩ·cm) was injected to fill the cell, and the ring-down lifetime τ was monitored as the solvent diffused into the polymer as shown in the inset of Figure 2. All EW-CRDS experiments and other investigations described in this paper were conducted at room temperature.

It was noted that cured PDMS films typically contain some residual non-cross-linked polymer as well as cross-linking catalyst; methanol is likely to extract these residues from the polymer films, whereas the hydrophobicity of PDMS should prevent this type of extraction by water.[31] Therefore, we completed a study in order to determine whether the presence of these substances has any effect on the shape of the EW-CRDS diffusion profile for methanol in the polymer. For these trials, PDMS films were prepared and cured in the same manner described above and then were treated with a solvent that is highly soluble in PDMS to remove these excess residues before EW-CRDS analysis. The films were soaked in toluene (Omnisolv) for approximately 3 h, during which time the toluene was replaced twice at 1-h intervals. The films were allowed to dry overnight and then were heated at 80 °C for ~30 min to drive off any excess toluene. These PDMS samples were then used for EW-CRDS analysis of methanol diffusion as described above.

To determine whether the general EW-CRDS trends seen are independent of wavelength, we completed a series of diffusion trials for methanol using 577-nm incident light from the same dye laser used for the previous measurements. The only change to the optical setup was the replacement of the 600-nm notch filter with a 577-nm notch filter (CVI Laser) following the second cavity mirror. The two wavelengths that were used are sufficiently far apart to demonstrate whether the results depend on any absorption features in the samples. The EW-CRDS trials conducted at this wavelength employed PDMS films that had been prepared as described above and not treated with toluene.

Weight-Gain Method. For comparison with the qualitative EW-CRDS studies, we conducted the traditional weight-gain method[32−34] on larger sheets of PDMS to monitor diffusion profiles and determine diffusion coefficients for methanol and water in this polymer. Sheets of cross-linked PDMS, 3.175 mm thick, were formed by pouring the degassed RTV mixture into a cleaned glass mold and then curing in an 80 °C oven for 3 h. Several (17 to 20) pieces of the sheets (~3.5 cm × 3.5 cm) were individually weighed and were then immersed in 60-mL jars of methanol or water at time $t = 0$. At a specific time interval, each sample was removed, blotted, and reweighed approximately 30 to 40 s after removal from the liquid.

We have observed by eye that this bulk polymer becomes optically cloudy as each of the solvents diffuses into it with time. Because the light scattering could affect the optical losses seen by EW-CRDS, we compared the transparency of the polymer/methanol to that of the polymer/water system. Pieces of these polymer sheets were digitally photographed after they had been immersed in the solvents for approximately 9 h in order to make this comparison. In addition, visible spectra from 400 to 800 nm were recorded with a UV−vis spectrophotometer (Varian, Cary 6000i) for pieces of these polymer sheets that had been soaked in the solvents for approximately 19.5 h.

Surface Plasmon Resonance Analyses. We carried out angle-resolved surface plasmon resonance (SPR) analyses in order to confirm the published refractive index of the PDMS samples and to elucidate the factors that contribute to the optical losses observed with EW-CRDS. We used a home-built SPR optical setup in the Kretschmann configuration, which has been described elsewhere.[35] A simple machined-glass flow cell was secured to the samples with pressure. The SPR substrates consisted of SF10 glass covered with an evaporated ~1-nm binding layer of Ti or Cr followed by a ~50-nm layer of Au; these substrates were index matched to an SF10 right-angle prism (CVI Laser) with index-matching fluid ($n = 1.730 \pm 0.0005$, R. P. Cargille Laboratories, Inc.). The PDMS samples for study were prepared on top of the gold surface using the spin-coating procedure described above, with the exception that the polymer was coated directly onto the SPR substrates and therefore was not transferred from microscope slide to substrate. In addition, most of the gold substrates were used as is for coating and were not cleaned with acetone or toluene. We recorded angle-resolved SPR curves for pure water, pure methanol, and PDMS films. In addition, we injected an aliquot of each solvent into the flow cell above the polymer and recorded SPR data at several time intervals while the methanol or water penetrated the polymer layer.

Film Thickness Measurements. We measured the thicknesses of all spin-coated films following the experimental trials; we used these measurements to determine whether differences in experimental diffusion profiles result from thickness differences from one film to another. Each film was cut vertically with a razor blade, and its cross section was suspended over the stage of a transmission microscope (Zeiss Axiovert 135) arranged to project onto a television screen. The width of the cross section as measured on the television screen was converted to microns by calibrating with a stage micrometer (Pyser-SGI Limited).

Results and Discussion

At first thought, it is not obvious that injection of a transparent solvent onto a transparent polymer film should produce large optical losses at the buried interface between the fused-silica substrate and the polymer. It was our initial intention to use the polymer/solvent system as a low-optical-loss background and then to monitor the diffusion of the biological dye trypan blue into the polymer in a manner similar to previous ATR studies.[36] As shown in the figures to follow, however, the simple permeation of PDMS by the solvent produces significant interfacial optical losses. It was anticipated that the mathematical relationship between these optical losses and the concentration of permeant would be straightforward and would therefore provide a means to calculate diffusion coefficients for methanol and water in PDMS, but this expectation proved false upon discovering that delamination of the film from the substrate makes a significant, if not dominant, contribution to the optical losses.

EW-CRDS Investigations. Figure 3a presents a representative EW-CRDS data set of ring-down lifetime τ versus time for injection of methanol above a ~208-μm-thick PDMS film. There are several interesting features to note about this plot. First, a lag time of approximately 5 min occurs between the injection of the methanol sample (at time $t = 0$) into the cell and the start of the sharp decrease in τ. We attribute this lag to the length of time required for methanol to penetrate the polymer layer and reach the interface to cause optical losses. In addition, there is a small increase in τ (from ~740 ns to ~768 ns) during

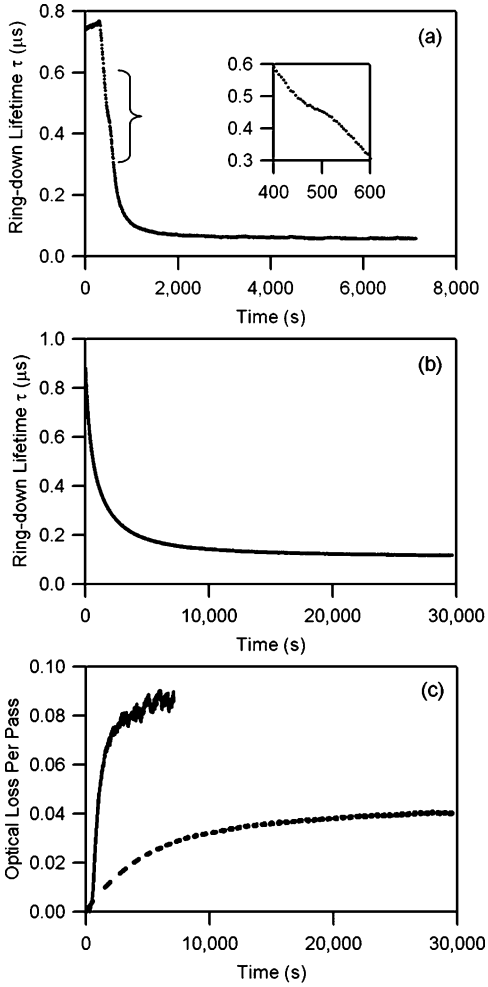

Figure 3. Representative plots of ring-down lifetime τ measured using 600-nm light versus time after injection of (a) methanol and (b) water above a PDMS film. Each data point is the average lifetime calculated over an interval of 5 s. The inset in panel a shows a magnification of the inflection point. Panel c shows interfacial optical loss per light pass versus time after injection of (−) methanol and (- -) water, analyzed from the data shown in panels a and b.

the first few minutes after injection. This increase is believed to be caused by pressure from the solvent injection or swelling of the polymer or both, which may improve the homogeneity of the contact between the polymer film and the prism and therefore reduce slightly scattering losses. The sharp decrease in τ indicates that methanol has reached the most intense region of the evanescent wave and has begun to cause optical losses at the prism/polymer interface. In addition, the inset in Figure 3a shows an enlargement of a section of the downward slope in which a slight inflection point appears. Although the exact cause of this feature is not known, it is believed that the inflection may be related to abrupt delamination of the PDMS layer from the prism surface as the PDMS swells slightly with methanol.

We recorded 10 data sets with initial τ values greater than 570 ns; the majority of these trials show both the initial increase following injection as well as the inflection point at approximately the same location in the downward slope. A few data sets, however, are smoother overall and either exhibit these features minimally or lack them entirely. These variations from one curve to the next probably result from differences in the quality of the PDMS/prism interface as also evidenced by differing initial τ values for all samples. Further investigation into preparative methods is necessary to improve the reproducibility of this optical interface. Despite these differences among the data sets, all methanol trials show similar lag times before the initial sharp decrease in τ. Moreover, they have essentially the same overall rates of change as well as similar equilibrium optical losses.

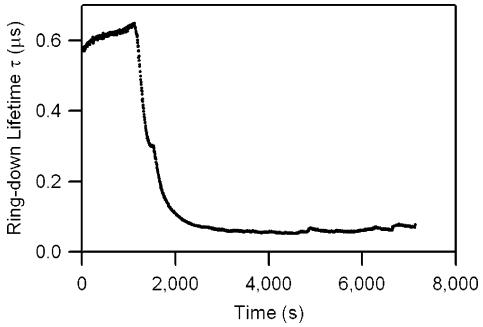

Figure 4. A representative plot of ring-down lifetime τ measured using 600-nm light versus time after injection of methanol above a toluene-treated PDMS film. Each data point is the average lifetime calculated over an interval of 5 s.

Figure 3b shows a representative plot of τ at 600 nm versus time for injection of water above a ~187-μm-thick PDMS film. A few notable differences are apparent between this behavior and the methanol data set shown in Figure 3a. First, this water plot shows a sharp decrease in τ almost immediately following injection of the water above the film. This behavior suggests that initially water penetrates PDMS much more rapidly than methanol, reaching the region of the interface in only a few seconds. Once the sharp decrease begins, however, the rate of change of τ is slower than that for the methanol system. The curve is very smooth and lacks the inflection point seen in the methanol plot. We recorded eight complete data sets for water injection. All show the rapid decrease within ~5 to 60 s as well as the smooth curve lacking the inflection point midway through the downward slope. Some, however, contain a small upward spike in τ after solvent injection and before the sharp decrease begins, as was seen for methanol. This trend is again attributed to inhomogeneities in the optical quality of the prism/polymer interface that could be altered by the pressure of solvent injection. The maximum in this upward spike was taken to be τ_0 in calculating the optical losses using eq 1.

Figure 3c shows the interfacial optical losses per pass, A^*, calculated from the data shown in Figure 3a,b. It is evident that after the first few minutes, the rate of change of optical losses for the methanol system far exceeds that for water. In addition, the absolute equilibrium A^* value for the methanol system is much greater than that for the water system, and it is reached more quickly than for water. Of the ten methanol trials discussed above, data were recorded for a sufficient period of time to calculate equilibrium optical loss values in seven cases; points between 5750 and 6750 s are averaged for the determination of the equilibrium τ value. From these seven data sets, we calculate A^* for the methanol/PDMS system to be 0.096 ± 0.005 (95% confidence). Of the eight water trials mentioned previously, one equilibrium value is discarded as an outlier with greater than 99% confidence. For the remaining seven trials, points between 17625 and 18625 s are averaged for the equilibrium τ value. We calculate the equilibrium A^* for the water/PDMS system to be 0.029 ± 0.005 (95% confidence).

Figure 4 shows representative data for ring-down lifetime τ at 600 nm after injection of methanol above a film that has been treated with toluene to extract cross-linking catalyst and non-cross-linked polymer that remained in the film after the curing process. The data set is somewhat noisier than that shown

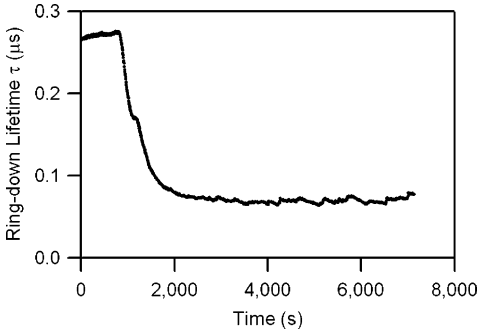

Figure 5. A representative plot of ring-down lifetime τ measured using 577-nm light versus time after injection of methanol above a PDMS film. Each data point is the average lifetime calculated over an interval of 5 s.

in Figure 3a; this noise may result from dust and other inhomogeneities at the polymer film surface that accumulated during the additional procedural steps. In addition, it may be noted that the lag time between injection of methanol and the start of the sharp decrease in τ is longer than that in Figure 3a; this result corresponds with the use of a significantly thicker ($\sim$348 μm) PDMS film for the toluene treatment procedure. Three methanol diffusion trials were conducted with toluene-treated films. With the exception of the explainable slight differences mentioned previously, the curve shapes for all three trials strongly resemble that in Figure 3a. In addition, A^* for methanol permeation of the toluene-treated films equals 0.10 $\pm$ 0.03 (95% confidence), which corresponds well with the calculated value for the untreated films. Thus, we conclude that the differences between the methanol diffusion curves and the water diffusion curves in Figure 3 do not result from the presence of extractable residues in the PDMS films.

From the EW-CRDS data in Figures 3a−c and 4 alone, it is not known which potential source of optical losses dominates in these studies. It is not expected that the optical losses seen at the polymer/prism interface during methanol or water diffusion result from the appearance of an absorption feature at 600 nm, because only a change in transparency, and not a color change, is evident by eye when a large piece of PDMS is soaked in either solvent. This supposition is tested by carrying out EW-CRDS measurements at 577 nm. Figure 5 plots τ versus time after injection of methanol onto PDMS. Not surprisingly, the ring-down lifetimes measured at this wavelength are much shorter than those observed at 600 nm, owing to the optimization of the prism and mirror coatings for 600 nm. The equilibrium A^* value at 577 nm is 0.061 $\pm$ 0.007, which differs somewhat from the A^* value at 600 nm; such a difference is to be expected, however, because the penetration depth and amplitude of the evanescent wave are affected by the wavelength in use.[21] Of primary importance is the fact that the general curve shape at 577 nm appears very similar to the curves obtained at 600 nm for methanol, within error. This result at a wavelength so far from 600 nm adds confidence to the assertion that the optical losses using CRDS are caused by a phenomenon other than 600-nm absorption.

Weight-Gain Method. The traditional weight-gain method lacks the spatial resolution inherent in our EW-CRDS method but allows us to quantify diffusion coefficients accurately for the permeation of bulk polymer samples by the solvents. This method provides a reliable comparison for the trends observed by EW-CRDS. Figure 6a shows representative weight-gain data sets for the diffusion of methanol and water into PDMS. Percent weight gain is plotted versus time at which each polymer piece was removed following immersion in the solvent. It is immediately evident that the weight-gain curves are quite smooth for both solvents and that methanol is about an order of magnitude more soluble in PDMS than water.

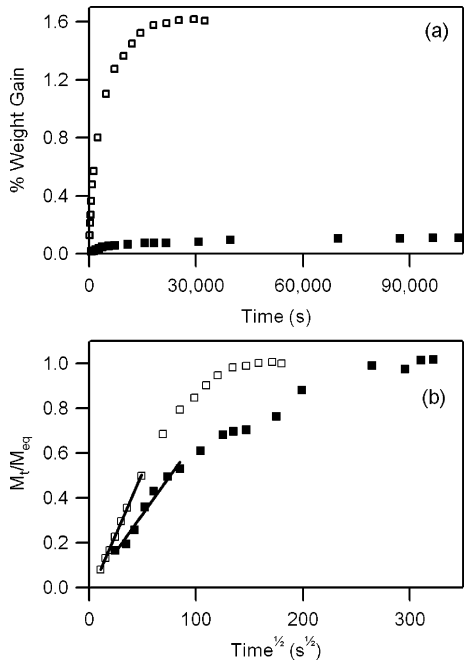

Figure 6. Representative data sets are shown in panel a for percent weight gain versus time for bulk measurements of diffusion through PDMS by (□) methanol and (■) water. The same data have been replotted in panel b to show normalized weight gain M_t/M_{eq} versus time$^{1/2}$ for diffusion of (□) methanol and (■) water to determine diffusion coefficients for the two solvents. For each data set, a line has been fit to all points for which $M_t/M_{eq} < 0.6$. For the methanol data, $R^2 = 0.999$ and $D = (25.1 \pm 0.7) \times 10^{-7}$, and for the water data $R^2 = 0.969$ and $D = (7 \pm 2) \times 10^{-7}$.

If the diffusion of each of these solvents obeys Fick's laws, diffusion through the plane polymer sheet can be described by the equation[32−34,37]

$$\frac{M_t}{M_\infty} = \frac{4}{l}\left(\frac{Dt}{\pi}\right)^{1/2} \qquad (2)$$

for the region in which the polymer has gained less than 60% of its equilibrium weight gain. Here M_t is the percent weight gain at time t, M_∞ is the percent weight gain at infinite time, l is the thickness of the polymer film, and D is the diffusion coefficient for penetration of the polymer by the solvent of interest. In this case, M_∞ is approximated as M_{eq}, the equilibrium percent weight gain that has been determined by the average of percent weight gain data points between 62 500 and 122 500 s for methanol and between 20 000 and 33 000 s for water. These are regions in time during which the percent weight gain levels off for each of the two systems, though the water/polymer system continues to increase in weight at a very slow rate for several days.

The data from Figure 6a are replotted in Figure 6b to show M_t/M_{eq} versus $t^{1/2}$ for the determination of methanol and water diffusion coefficients. The larger noise in the water plot results from the smaller weight gains that have been measured. The good linearity of both plots below $M_t/M_{eq} = 0.6$ indicates that the diffusion is Fickian and that on average methanol diffuses significantly more quickly than water in cross-linked PDMS. Three data sets were collected for each system. D is calculated with 95% confidence to be (25.1 $\pm$ 0.7) $\times$ 10^{-7} cm^2/s for methanol in PDMS and (7 $\pm$ 2) $\times$ 10^{-7} cm^2/s for water in

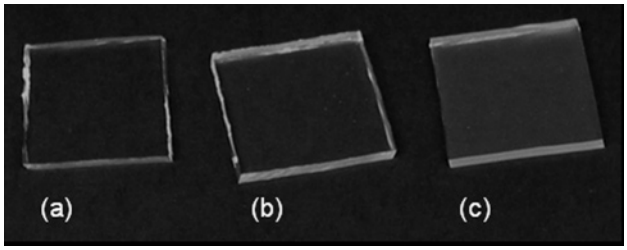

Figure 7. A photograph taken of three pieces of 3.175-mm-thick PDMS: (a) dry; (b) after soaking in methanol for 9 h, 2 min; and (c) after soaking in water for 9 h, 2 min. The photograph was taken approximately 33 s after removal of pieces "b" and "c" from the solvents, during which time they were blotted dry.

PDMS, both of which are comparable to *D* values that have been reported by several other groups for small protic solvents in PDMS.[38] A few groups have reported *D* values for water that are approximately an order of magnitude larger than those measured in this study;[39] these differences may result from variations in the polymer structure such as the omission of cross-linking.

These weight-gain results generally confirm the EW-CRDS results discussed above. The greater solubility for methanol in PDMS corresponds qualitatively with the greater optical losses that were observed for the methanol system with EW-CRDS. The larger *D* value for methanol calculated with the weight-gain method also agrees with the greater average rate of change for the methanol data in EW-CRDS. In addition, both techniques indicate that methanol uptake into PDMS levels off about three times as fast as water uptake. Not surprisingly, the EW-CRDS observation that water uptake is faster than methanol uptake at short times is neither confirmed nor refuted by the weight-gain data, because the weight-gain experiments are time-limited. The tiny weight increases that occur in the first few minutes after immersion are very difficult to measure accurately. In addition, a small amount of liquid evaporates for the ~30 s required to blot the PDMS samples and transfer them to the analytical balance. For these reasons, weight-gain measurements were taken no more often than every few minutes, whereas the EW-CRDS measurements have been averaged every 5 s.

Additional experimental results help to elucidate the source of the interfacial optical losses observed with EW-CRDS for these polymer/solvent systems. Figure 7 is a photograph of three pieces of PDMS that are similar in size to those used for the weight-gain method. Piece "a" is dry, piece "b" has been soaked in methanol for 9 h and 2 min, and piece "c" has been soaked in water for the same period of time. This photograph demonstrates that the polymer/water system is slightly more opaque than both the dry polymer system and the polymer/methanol system after several hours of immersion in solvent.

Figure 8 shows visible spectra of similar PDMS pieces that have been immersed in the solvents for approximately 19.5 h. These spectra show again that the optical losses are greater for the water-soaked polymer than for the methanol-soaked piece, and the spectra also corroborate the earlier suggestion that the losses in these polymer/solvent systems result from scattering and not absorption. There are no distinct absorption peaks, and the measured losses increase with increasing energy (decreasing wavelength). This opacity, or optical scattering, that results from uptake of solvent must be one contributor to the optical losses seen at the polymer/prism interface in the EW-CRDS experiments. It cannot be the dominating factor, however, because it does not explain the vastly greater optical losses seen with EW-CRDS for the methanol system in comparison with the water

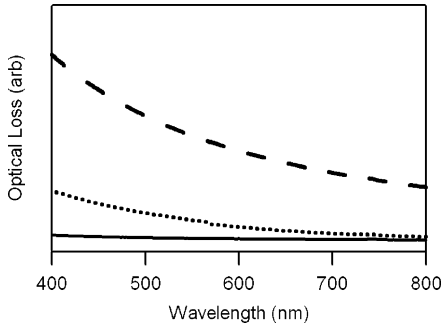

Figure 8. Visible spectra of three pieces of 3.175-mm-thick PDMS (—) dry, (•••) after soaking in methanol for ~19.5 h, and (- - -) after soaking in water for ~19.5 h. These spectra were taken approximately 30 s after removal of the pieces from the solvents, during which time they were blotted dry.

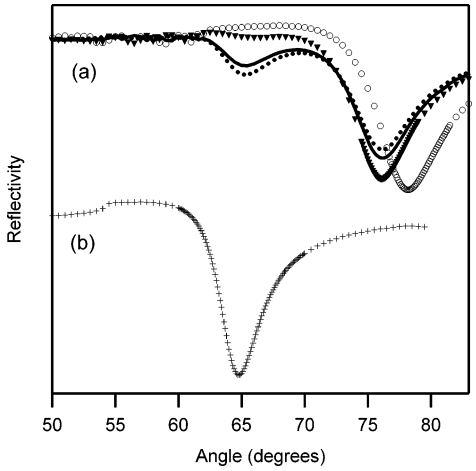

Figure 9. Angle-resolved surface plasmon resonance curves for diffusion of methanol through a PDMS film are shown in panel a. Individual curves show the SPR signal for a ~92-μm-thick film of PDMS: (○) before injection of methanol; (▼) ~3 min, 38 s after injection of methanol; (—) ~14 min, 37 s after injection; and (●) ~53 min, 22 s after injection. A representative angle-resolved SPR scan is plotted in panel b for pure methanol with no PDMS layer present.

system. This conclusion makes us suspect that film delamination at the interface might be playing a significant role. The SPR study we describe next confirms this suspicion.

Surface Plasmon Resonance Study. A representative angle-resolved SPR curve for a PDMS film (○) is shown at the far right of Figure 9a. The position of the SPR angle near 78° is, within error, what is expected from the published refractive index[40] of 1.406. The other curves in Figure 9a show SPR data for the PDMS system at three time intervals after injection of methanol above the film. The fact that the curves do not shift to the right (and even shift slightly to the left) illustrates that, as expected, the PDMS refractive index does not increase with permeation of the lower-refractive-index solvent methanol. We conclude that the incident angle used for the light in the EW-CRDS apparatus has been sufficient for TIR throughout the duration of the experiments, and therefore incomplete total internal reflection is not the cause of the optical losses observed with EW-CRDS. The left shift of the PDMS peak results from either a decrease in the refractive index of the solvent-soaked PDMS or an insertion of a thin (<100 nm), homogeneous layer of methanol that has permeated the PDMS and separates the prism from the polymer layer, or the shift possibly results from a combination of both phenomena.

Most notably, a second peak grows in with time after injection of the methanol aliquot. This peak occurs at the same angle as

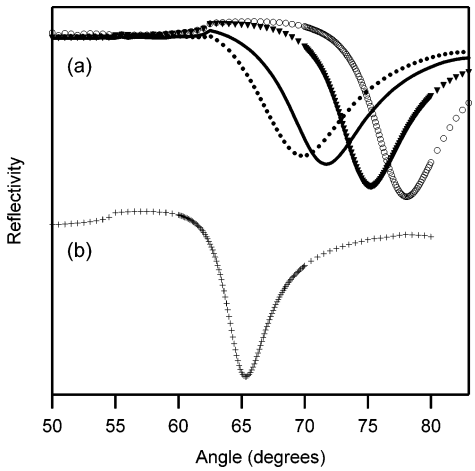

Figure 10. Angle-resolved surface plasmon resonance curves for diffusion of water through a PDMS film are shown in panel a. Individual curves show the SPR signal for a ~93-μm-thick film of PDMS: (○) before injection of water; (▼) ~4 min, 46 s after injection of water; (−) ~59 min, 25 s after injection; and (●) ~169 min, 37 s after injection. A representative angle-resolved SPR scan is plotted in panel b for pure water with no PDMS layer present.

the pure methanol SPR angle, shown for comparison in Figure 9b. The presence of two SPR peaks in a single angle-resolved curve is very uncommon and indicates that two distinct populations of molecules must be present and horizontally separate from one another above the illumination region (~1 mm^2) of the substrate. The peak at ~65° gives evidence that in an area of the illumination region, the PDMS has been delaminated from the substrate surface to the extent that only bulk methanol covers the region of the evanescent field above the SPR substrate. This delamination is attributed to slight swelling and penetration of the polymer by the solvent. The polymer layer is constrained around the edges by the pressure of the flow cell; therefore, when it swells with solvent, it is likely to lift off of the surface of the substrate. The remaining peak at ~75° shows that some PDMS still remains attached directly to the SPR substrate surface or has been delaminated only slightly by a thin, homogeneous layer of methanol.

The angle-resolved SPR curves for injection of water onto the PDMS film have a significantly different appearance. As was seen in Figure 9a, the far-right curve in Figure 10a depicts the expected SPR curve for PDMS. Following the injection of water, the SPR peak shifts to the left, but the characteristic peak for water at 65° does not appear, which means that the system above the SPR substrate consists only of a single population of molecules that is homogeneous in the horizontal plane above the illumination region. This single peak is attributed to a PDMS layer that has been separated slightly from the SPR substrate by a thin layer of water (~50−100 nm) but that has not been completely delaminated to allow a region of bulk water to grow in. The homogeneity of the system is attributed to the fact that water solubility in PDMS is sufficiently low to cause minimal swelling of the polymer layer.

We conducted at least three SPR trials for the injection of both water and methanol onto PDMS films. From one trial to the next, the extent to which the peaks shift and the relative sizes of the peaks vary; however, two SPR peaks appear for all methanol trials, in contrast to one peak for all water trials. These results clearly show that the mechanical processes at the PDMS/substrate interface during penetration by solvent differ greatly for methanol and water. On the basis of these differences, we conclude that the inhomogeneous delamination of the polymer by methanol is the cause of significant scattering of the evanescent field in EW-CRDS, whereas the homogeneous formation of a solvent layer in the water system does not attenuate the evanescent field to the same extent. These results suggest that the mathematical relationship of the interfacial optical losses to the concentration of permeant is not straightforward as it would be if the losses were dominated by a simple absorption phenomenon. Therefore, we are currently prevented from quantifying the diffusion coefficients for methanol and water in PDMS using EW-CRDS.

These conclusions about the delamination of the PDMS from the prism surface point to another potential application of the EW-CRDS technique. Investigators might employ this method to measure the quality of different chemical and mechanical methods for adhering a polymer layer to a glass substrate such as the prism used here. They could inject a solvent sample above the polymer layer and monitor the ring-down lifetime as was done in this study. The magnitude of the measured optical losses should reflect the extent to which the polymer layer becomes delaminated from the prism and could guide investigators to choose the preparative method with the most desirable adherence characteristics. A perfectly adhered polymer layer should exhibit minimal interfacial optical losses in comparison with those observed in this study. The suggested directions mentioned here are only a couple of the many possibilities that remain open for the application of EW-CRDS to investigate interfacial phenomena.

Summary and Conclusions

In this study, we have employed evanescent-wave cavity ring-down spectroscopy to monitor optical losses at a polymer/prism interface as solvents diffuse into the polymer. We have characterized the types of information that can be gained from such investigations, and we have determined the dominating source of the optical losses that are observed for this system.

The EW-CRDS data have indicated that methanol uptake is slower than water uptake in the first few minutes after injection of solvent above the layer of cross-linked PDMS, but that after this time period methanol diffuses much more quickly on average. This comparison of relative average diffusion rates has been confirmed by the bulk weight-gain technique. In addition to the relative diffusion rates, the significantly greater equilibrium optical losses seen with EW-CRDS for the methanol system correspond qualitatively with the larger solubility of methanol in PDMS. Further experimentation is clearly necessary to confirm whether this technique provides reasonable estimates for systems that differ from those examined here; however, based upon the results shown here, the EW-CRDS technique shows promise as a tool for the comparison of relative diffusion rates and solubilities for polymer/solvent systems. Whereas the bulk weight-gain method provides more accurate quantification of D values, it is limited by the need for large samples in order to obtain detectable changes in weight, the low time resolution inherent in the removal and weighing process, and a lack of spatial resolution. The EW-CRDS technique provides information in real time, with small samples, and with greater spatial resolution. These advantages could be particularly useful for the analysis of microfluidic lab-on-a-chip devices, in which different channels of a single chip might be chemically treated to alter diffusion properties.

We have succeeded in obtaining information about the source of the EW-CRDS interfacial optical losses through the use of several other investigations. The demonstration of similar EW-CRDS results at a significantly different wavelength and the

visible spectra of solvent-soaked PDMS samples have shown that the optical losses are not caused by the presence of an unexpected absorption feature in the chemical system. The examination of bulk PDMS transparency, as evidenced by the photograph and the visible spectra, has suggested that optical scattering throughout the bulk PDMS resulting from uptake of solvent is a probable contributor to the EW-CRDS losses. This scattering cannot be the main contributor, however, because the PDMS/water system appears more opaque, but the EW-CRDS losses are greater for methanol. The SPR investigations of solvent penetration of PDMS have provided strong evidence to show that methanol permeates and swells the polymer enough to create pockets of bulk methanol at the interface, whereas water forms a homogeneous, thin film at most between the substrate and the polymer. We believe that the nature of the delamination causes nonuniformities at the polymer/substrate interface that attenuate the EW-CRDS signal significantly and therefore dominate the EW-CRDS interfacial optical losses.

Acknowledgment. The authors would like to thank Curtis Frank for use of the SPR apparatus in his laboratory. Hongkai Wu and Gabriele Trapp provided valuable insights about the properties of PDMS. This material is based upon work supported by the National Science Foundation under Grant Nos. MPS-0313996 and PHY-0411641.

References and Notes

(1) O'Keefe, A.; Deacon, D. A. G. *Rev. Sci. Instrum.* **1988**, *59*, 2544−2551.
(2) Berden, G.; Peeters, R.; Meijer, G. *Int. Rev. Phys. Chem.* **2000**, *19*, 565−607.
(3) Atkinson, D. B. *Analyst* **2003**, *128*, 117−125.
(4) Zalicki, P.; Zare, R. N. *J. Chem. Phys.* **1995**, *102*, 2708−2717.
(5) Curran, R. M.; Crook, T. M.; Zook, J. D. *Mater. Res. Soc. Symp. Proc.* **1988**, *105*, 175−180.
(6) Engeln, R.; Berden, G.; van den Berg, E.; Meijer, G. *J. Chem. Phys.* **1997**, *107*, 4458−4467.
(7) Pipino, A. C. R.; Hudgens, J. W.; Huie, R. E. *Chem. Phys. Lett.* **1997**, *280*, 104−112.
(8) Kleine, D.; Lauterbach, J.; Kleinermanns, K.; Hering, P. *Appl. Phys. B* **2001**, *72*, 249−252.
(9) Gupta, M.; Jiao, H.; O'Keefe, A. *Opt. Lett.* **2002**, *27*, 1878−1880.
(10) Hallock, A. J.; Berman, E. S. F.; Zare, R. N. *Anal. Chem.* **2002**, *74*, 1741−1743.
(11) von Lerber, T.; Sigrist, M. W. *Appl. Opt.* **2002**, *41*, 3567−3575.
(12) Xu, S. C.; Sha, G. H.; Xie, J. C. *Rev. Sci. Instrum.* **2002**, *73*, 255−258.
(13) Muir, R. N.; Alexander, A. J. *Phys. Chem. Chem. Phys.* **2003**, *5*, 1279−1283.
(14) Shaw, A. M.; Hannon, T. E.; Li, F.; Zare, R. N. *J. Phys. Chem. B* **2003**, *107*, 7070−7075.
(15) Snyder, K. L.; Zare, R. N. *Anal. Chem.* **2003**, *75*, 3086−3091.
(16) Tong, Z. G.; Jakubinek, M.; Wright, A.; Gillies, A.; Loock, H. P. *Rev. Sci. Instrum.* **2003**, *74*, 4818−4826.
(17) Pipino, A. C. R.; Woodward, J. T.; Meuse, C. W.; Silin, V. *J. Chem. Phys.* **2004**, *120*, 1585−1593.
(18) Stewart, G.; Atherton, K.; Yu, H. B.; Culshaw, B. *Meas. Sci. Technol.* **2001**, *12*, 843−849.
(19) Smets, A. H. M.; van Helden, J. H.; van de Sanden, M. C. M. *J. Non-Cryst. Solids* **2002**, *299/302*, 610−614.
(20) Tarsa, P. B.; Rabinowitz, P.; Lehmann, K. K. *Chem. Phys. Lett.* **2004**, *383*, 297−303.
(21) Harrick, N. J. *Internal Reflection Spectroscopy*; Wiley & Sons: New York, 1967.
(22) *Internal Reflection Spectroscopy*: *Theory and Applications*; Marcel Dekker: New York, 1992; Vol. 15.
(23) Umemura, T.; Kasuya, Y.; Odake, T.; Tsunoda, K. *Analyst* **2002**, *127*, 149−152.
(24) Pipino, A. C. R. *Phys. Rev. Lett.* **1999**, *83*, 3093−3096.
(25) Pipino, A. C. R. *Appl. Opt.* **2000**, *39*, 1449−1453.
(26) Pipino, A. C. R.; Hoefnagels, J. P. M.; Watanabe, N. *J. Chem. Phys.* **2004**, *120*, 2879−2888.
(27) Li, F.; Zare, R. N. *J. Phys. Chem. B* **2005**, *109*, 3330−3333.
(28) Tarsa, P. B.; Wist, A. D.; Rabinowitz, P.; Lehmann, K. K. *Appl. Phys. Lett.* **2004**, *85*, 4523−4525.
(29) Wheeler, A. R.; Throndset, W. R.; Whelan, R. J.; Leach, A. M.; Zare, R. N.; Liao, Y. H.; Farrell, K.; Manger, I. D.; Daridon, A. *Anal. Chem.* **2003**, *75*, 3249−3254.
(30) Wheeler, A. R.; Leach, A. M.; Trapp, G. S. Personal communication.
(31) Wu, H. Personal communication.
(32) Crank, J. *The Mathematics of Diffusion*, 2nd ed.; Oxford University Press: New York, 1975.
(33) Britton, L. N.; Ashman, R. B.; Aminabhavi, T. M.; Cassidy, P. E. *J. Chem. Educ.* **1988**, *65*, 368−370.
(34) Vergnaud, J. M. *Liquid Transport Processes in Polymeric Materials*; Prentice Hall: Englewood Cliffs, NJ, 1991.
(35) Bailey, L. E.; Kambhampati, D.; Kanazawa, K. K.; Knoll, W.; Frank, C. W. *Langmuir* **2002**, *18*, 479−489.
(36) Elabd, Y. A.; Baschetti, M. G.; Barbari, T. A. *J. Polym. Sci., Part B*: *Polym. Phys.* **2004**, *42*, 365.
(37) Balik, C. M. *Macromolecules* **1996**, *29*, 3025−3029.
(38) Duineveld, P. C.; Lilja, M.; Johansson, T.; Inganas, O. *Langmuir* **2002**, *18*, 9554−9559 and references therein.
(39) Fritz, L.; Hofmann, D. *Polymer* **1997**, *38*, 1035−1045 and references therein.
(40) Information obtained from the GE Silicones website, http://www.gesilicones.com.